



## RNA sequencing analysis of early-stage atherosclerosis in vascular-on-a-chip and its application for comparing combustible cigarettes with heated tobacco products

Kazuhiro Ohashi<sup>1</sup>, Ayaka Hayashida<sup>1</sup>, Atsuko Nozawa, Shigeaki Ito<sup>\*</sup>

Scientific Product Assessment Center, Japan Tobacco Inc., 6-2, Umegaoka, Aoba-ku, Yokohama, Kanagawa 227-8512, Japan

### ARTICLE INFO

#### Keywords:

Atherosclerosis  
Organ-on-a-Chip  
Next generation sequencing  
Macrophages  
Heated tobacco products  
Pathway analysis

### ABSTRACT

Our previous study showed promising results in replicating early-stage atherosclerosis when vascular endothelial cells (VECs) were exposed to cigarette smoke (CS) extract via M0 macrophages. We used an organ-on-a-chip system as an alternative to animal testing to model atherosclerosis, which is a complex disease involving endothelial and immune cell communications. By incorporating macrophages into the vascular-on-a-chip system, we aimed to mimic the indirect effects of inhalable substances, such as CS, on VECs. In the current study, we further examined the suitability of our *in vitro* system for mimicking early-stage atherosclerosis by transcriptomic analyses of VECs exposed to CS directly or indirectly via macrophages. We also incorporated M1 macrophages to replicate a preexisting inflammatory state. We found a greater number of differentially expressed genes (DEGs) in direct exposure methods than indirect exposure methods. However, a pathway analysis showed that the direct exposure of CS to VECs primarily caused cell death-related pathway alterations, and the “Atherosclerosis Signaling” pathway was predicted to be negatively regulated. Indirect exposure via M0 macrophages similarly showed that the identified DEGs were related to cell death, while the “Atherosclerosis Signaling” pathway was predicted to be activated. In contrast, cell death-related pathway alterations were not observed by indirect exposure of CS to VECs via M1 macrophages, but the pathway perturbations were similar to a pro-inflammatory positive control. In addition, the “Atherosclerosis Signaling” pathway was predicted to be activated in VECs that were indirectly exposed to CS via M1 macrophages. These results suggest that M0 or M1 macrophages contribute to atherogenic transcriptomic changes in VECs, although they affect cell death-related pathways differently. We also used indirect exposure methods to compare the effects of CS and heated tobacco product (HTP) aerosol. Notably, gene expression changes related to atherosclerosis were less pronounced in HTP aerosol-exposed VECs than CS. Our study highlights the utility of the vascular-on-a-chip system with indirect exposure of CS extract via macrophages for replicating atherogenesis and suggests a reduced risk potential of the HTP. This research contributes to advancing alternatives to animal testing for toxicological and disease modeling studies.

### Introduction

Cardiovascular disease (CVD) is a general term for disorders of the cardiovascular system, and it is a leading cause of worldwide deaths (World Health Organization. Global health estimates: Leading causes of death., 2020). CVD generally involves atherosclerosis where abnormalities and narrowing of blood vessels occur. The accumulation of

immune cells, lipids, and extracellular matrices is found in such atheromatous lesions (Libby, 2019). The development of atheromatous lesions is normally initiated by impairment of vascular endothelium. Failure of barrier function, upregulation of adhesion molecules, and recruitment of blood immune cells are major initiating process of atherosclerosis (so-called endothelial dysfunction) (Gimbrone and Garcia-Cardena, 2016). The causes of endothelial dysfunction as well as

**Abbreviations:** VEC, vascular endothelial cell; CS, cigarette smoke; HTP, heated tobacco product; ROS, reactive oxygen species; DT3.0a, Direct Heating Tobacco System Platform 3 Generation 3 version a; DEG, differentially expressed gene; HCAEC, human coronary artery endothelial cell; TPM, total particulate matter; ACM, aerosol collected mass; IPA, ingenuity pathway analysis.

\* Corresponding author.

E-mail address: [shigeaki.ito@jt.com](mailto:shigeaki.ito@jt.com) (S. Ito).

<sup>1</sup> Kazuhiro Ohashi and Ayaka Hayashida contributed equally to this work.

<https://doi.org/10.1016/j.crttox.2024.100163>

Received 17 December 2023; Received in revised form 27 February 2024; Accepted 19 March 2024

Available online 21 March 2024

2666-027X/© 2024 The Authors. Published by Elsevier B.V. This is an open access article under the CC BY-NC-ND license (<http://creativecommons.org/licenses/by-nc-nd/4.0/>).

CVD are multifactorial and include an unhealthy dietary habit, alcohol consumption, and a lack of exercise, and these causes are interrelated (Raffeian-Kopaei, 2014). Protein carbonylation, lipid peroxidation, ethanol metabolism, and deterioration of antioxidant capacity are commonly induced by such lifestyle habits, and they directly contribute to induce oxidative conditions in the vasculature, leading to endothelial dysfunction (Lesgards, 2002; Obad, 2018; Salekeen, 2022; Ou, 2017). Cigarette smoking also causes oxidative stress. Various studies have shown that CS and its extract cause production of intracellular reactive oxygen species (ROS), glutathione depletion, and nuclear factor-erythroid 2-related factor 2 activation (Gould, 2011; Sekine, 2019). When smoking occurs, CS is not directly exposed to the vascular endothelium but via inhalation through the respiratory tract. Therefore, the effects of CS on the vascular endothelium appear to occur by the constituents in smoke or their metabolites that pass through the lungs, and various mediators secreted from immune cells in the respiratory tract (Kotlyarov, 2023) (Borger, 2020). Tissue-resident macrophages, such as alveolar macrophages and interstitial macrophages, play a role in innate immunity, which includes inflammatory responses (Lugg, 2022; Aegerter et al., 2022). Such tissue-resident macrophages typically show heterogeneity regarding their subtype that contributes to maintain tissue homeostasis (Hou, 2021). The classical activation of macrophages into the M1 subtype causes secretion of inflammatory cytokines, and CS is one of its known inducers (Yang and Chen, 2018). Therefore, such active metabolites of smoke constituents and cytokines may influence vascular inflammation via their transport into the blood stream.

Harmful and potentially harmful constituents (HPHCs) (Food, 2012) in CS are considered to cause oxidative stress and inflammatory responses (Horinouchi, 2020; Zhou, 2022; Shi et al., 2021). Therefore, reducing exposure to HPHCs is a way to reduce such adverse biological events, could thus potentially contribute to reduce risk of inflammatory diseases including atherosclerosis. Recently, several types of tobacco products, such as e-cigarettes and heated tobacco products (HTPs), have become popular. They generally emit aerosol with less and fewer chemical constituents than combustible cigarettes, and thus they are expected to be reduced-risk products (Hashizume, 2023; Forster, 2018). The US Food and Drug Administration (FDA) has issued an order of modified risk tobacco products if the applicant has demonstrated that the product, as it is actually used by consumers, will significantly reduce harm and the risk of tobacco-related disease to individual tobacco users, and benefit the health of the population under section 911(g)(1) of the FD&C Act (Food and Drug Administration, Modified Risk Tobacco Product Applications DRAFT GUIDANCE., 2012). To date, several tobacco products have been granted a modified risk tobacco product order by the US FDA, in which one of the in-market HTPs (i.e., exposure modification order for IQOS) is included (Food and Drug Administration, Modified Risk Granted Orders., 2023). Because various HTPs are currently available and they differ from IQOS in certain aspect, the actual risk of HTPs, as a category of tobacco products, still needs to be investigated from the perspectives of both individual health risk and the potential health-benefit for the population as a whole.

Various studies have been conducted to estimate the potential risk of HTPs. The main interests of researchers regarding HTPs are the toxicological concerns and their risk in the respiratory tract (Dempsey, 2023; Saha, 2023; Muratani, 2023) because HTPs are inhalable products and have similar behavior of use as cigarettes. To date, several reports related to the reduced risk potential of HTPs for CVD have been published. Philips et al reported that atherosclerotic plaque formation was less accelerated in HTP aerosol-exposed mice (i.e., THS2.2) than CS-exposed mice, and that this was similar to Sham-exposed mice (Philips, 2019). In addition, Poussin et al reported that the extract of THS2.2 aerosol showed less pronounced effects than CS on monocyte-endothelial adhesion and expression of adhesion molecules (Poussin, 2016), which are known to be associated with the initiation of atherosclerosis. We also found that representative HTPs currently marketed in Japan, including THS and our proprietary Direct Heating Tobacco

System Platform 3 Generation 3 version a (DT3.0a), similarly showed reduced effects on the expression of adhesion molecules and monocyte adhesion *in vitro* when compared to CS (Ohashi, 2023). In our previous study, we constructed an assay system for early-stage atherosclerosis by using pseudo-co-culture of vascular-on-a-chip and macrophages (i.e., indirect exposure method via macrophages) (Ohashi, 2023). Briefly, CS-total particulate matter (TPM) or DT3.0a-aerosol-collected mass (ACM) was first exposed to macrophages, and then conditioned medium was subjected to the vascular-on-a-chip. In doing so, cell-cell communication between tissue-resident macrophages and the vascular endothelium could be reflected. Although a reduced-risk potential of DT3.0a was found with this assay system, whether it accurately resembles the atherogenic situation in human vasculature and the detailed mechanism underlying the reduced effects of DT3.0a aerosol on early-stage atherosclerosis are unclear. In addition, we used M0 macrophages in our previous study because we hypothesized a steady state of macrophages in healthy subjects. However, because of the situation in hyperlipidemia, which is a major risk factor for atherosclerosis, conditions of the blood are more likely to induce the M1 subtype because numerous proinflammatory cytokines and oxidative stress could be induced (Mishra and Prasad, 2022).

In this study, we aimed to examine the effectiveness of pseudo-co-culture of M1 macrophages to simulate atherosclerotic reactions under preexisting inflammatory conditions in vascular-on-a-chip, and to investigate the potential of this system for comparative risk assessment of DT3.0a aerosol. We also performed pseudo-co-culture of M0 macrophages with the same method used in our previous study and direct exposure of CS-TPM or DT3.0a-ACM to the vascular-on-a-chip (Ohashi, 2023). To investigate the appropriateness of pseudo-co-culture of M0 or M1 macrophages with vascular-on-a-chip, we used RNA sequencing (RNA-seq) analysis and pathway analysis of identified DEGs to investigate the biological perturbations and the resemblance of this model to atherogenesis. Analyses of DT3.0a-aerosol-exposed vascular-on-a-chip are expected to identify the underlying mechanism of the reduced risk potential of DT3.0a that we found in our previous study (Ohashi, 2023).

## Materials and methods

We used basically the same testing procedure as that in our previous study (Ohashi, 2023), but added pseudo-co-culture of M1 macrophages and the RNA-seq analysis.

### Subculture of arterial endothelial cells and THP-1 cells

Primary human coronary artery endothelial cells (HCAECs) and a human acute monocytic leukemia cell line (THP-1 cells) were subcultured before their application to an organ-on-a-chip platform (i.e., OrganoPlate, Mimetas, Leiden, The Netherlands; details are provided in the following subsection) as we reported previously (Ohashi, 2023). Briefly, HCAECs were purchased from PromoCell (Heidelberg, Germany) and cultured in a collagen I-coated flask (Corning, Corning, NY, USA) with the endothelial cell growth medium MV2 (Promocell) with a 1 % penicillin-streptomycin solution (Fujifilm Wako Pure Chemical Corporation, Osaka, Japan). THP-1 cells were purchased from the American Type Culture Collection (Manassas, VA, USA) and cultured in uncoated tissue culture flasks (Corning) with Roswell Park Memorial Institute 1640 medium (RPMI 1640) (Thermo Fisher Scientific, Waltham, MA, USA) containing fetal bovine serum (FBS) (Thermo Fisher Scientific) and a 1 % penicillin-streptomycin solution.

### OrganoPlate culture

Cell culture in OrganoPlate was performed using the same procedure that we reported previously (Ohashi, 2023). Two-lane OrganoPlate (Mimetas) was used in this study. Before seeding, 50  $\mu$ L of Hank's balanced salt solution (Thermo Fisher Scientific) was dispensed into the

**Table 1**

Brief summary of the exposure condition.

Conc.	1R6F			DT3.0a			NC	PC
	100 µg/ml	200 µg/ml	400 µg/ml	200 µg/ml	1000 µg/ml	3000 µg/ml	1 % DMSO	TNF + IL-1b
Direct	✓	✓	✓	✓	✓	✓	✓	✓
Indirect M0	✓	✓	✓	✓	✓	✓	✓	–
Indirect M1	✓	✓	✓	✓	✓	✓	✓	–

NC: negative control, PC: positive control

observation window to obtain optical clarity. A volume of 2 µL of gel composed of 3 mg/mL type 1-A collagen I, which was derived from a porcine tendon (Nitta Gelatin, Osaka, Japan), 10 × minimum essential medium Hank's culture medium (Nitta Gelatin), and reconstitution buffer (Nitta Gelatin) was then dispensed in the gel inlet. The gel was incubated for 15–30 min at 37 °C with 5 % CO<sub>2</sub> to complete gelation of the extracellular matrix. Each constituent was gently mixed well at a ratio of 8:1:1 (v/v) to prepare 100 µL of gel in the microtube each time. The tube was placed on ice and the mixed gel was used within 15 min. HCAECs at passages three to six were detached from flasks using 0.25 % Trypsin-EDTA (Thermo Fisher Scientific) and dispensed in MV2 medium at 5 × 10<sup>6</sup> cells/mL. A volume of 2 µL of cell suspension was then applied to the medium inlet. After cell seeding, 50 µL of MV2 medium was added to the medium inlet. The plate was incubated on its side for 3 h to allow the cells to attach to the extracellular matrix. Subsequently, 50 µL of MV2 medium was dispensed in the medium outlet, and the plate was placed on an Mimetas Rocker (Mimetas) in an incubator. The rocker was set at a 7° angle, and it was inverted every 8 min to reproduce bidirectional flow in the perfusion channel of the plate. The plate was cultured for 3–4 days until the formation of tubule structures.

#### Preparation of CS and DT3.0a aerosol extracts

To expose endothelial cells in the OrganoPlate, CS and DT3.0a aerosol extracts were prepared as described previously (Ohashi, 2023). A reference conventional cigarette and a DT3.0a were used in this study. Kentucky reference 1R6F cigarettes were purchased from the University of Kentucky, Kentucky Tobacco Research and Development Center (Lexington, KY, USA) and stored at below 4 °C until use. Our proprietary DT3.0a with one representative regular tobacco flavor stick was purchased from the Japanese market. The reference conventional cigarettes and tobacco sticks of DT3.0a were stored for at least 48 h at 22 °C ± 1 °C with 60 % ± 3 % relative humidity in accordance with the International Organization for Standardization (ISO) 3402 standard (Wickham, 2009). The battery of the heating device was fully charged prior to aerosol generation. Mainstream 1R6F CS and aerosol from DT3.0a were generated by an RM20H smoking machine (Borgwaldt KC, Hamburg, Germany). 1R6F CS was generated under International Organization for Standardization 20,778 (55 mL of puff volume, 30-s puff interval, 2-s puff duration, bell-shaped puff profile, and 100 % blocked ventilation holes) (Warnes, 2022), and TPM was collected on a 44-mm Cambridge filter pad. Aerosol of DT3.0a was generated in the same manner, but without blocking the ventilation holes, and ACM was collected on a 44-mm Cambridge filter pad. The reason for not blocking the ventilation holes was the positions of the holes inside the device, which precluded the possibility of blocking ventilation holes under the intended conditions of use. The pad was extracted with dimethyl sulfoxide (DMSO) purchased from Sigma-Aldrich (St. Louis, MO, USA) or Fujifilm Wako Pure Chemical Corporation to prepare a 40 mg/mL TPM solution for 1R6F (accumulated from 10 sticks) and a 200 mg/mL ACM solution for DT3.0a (10 sticks). The TPM and ACM solutions were stored at – 80 °C until testing.

#### Preparation of conditioned medium from THP-1-derived macrophages

The preparation of conditioned medium was also performed mostly

using the same procedure in our previous study (Ohashi, 2023). Briefly, TPM and ACM solutions were diluted to 100, 200, and 400 µg/mL and 200, 1000, and 3000 µg/mL, respectively, by adding MV2 medium to prepare TPM and ACM samples. Each sample was 1 % (TPM: 100, 200, and 400 µg/mL; ACM: 200 and 1000 µg/mL) or 1.5 % (ACM: 3000 µg/mL) adjusted with DMSO. The exposure concentrations were determined not to exceed a final concentration of DMSO at 1 % in the exposure medium to avoid unexpected effects caused by DMSO. Additionally, to investigate whether a much higher concentration of ACM exerts biological effects, we also used 3000 µg/mL ACM with 1.5 % DMSO. We confirmed in our previous study that TPM and ACM at these concentrations, as well as 1 % or 1.5 % DMSO alone, did not show obvious cytotoxicity (Ohashi, 2023). Differentiation of THP-1 into macrophages was performed with Advanced RPMI1640 (Thermo Fisher Scientific) containing 1 % fetal bovine serum and a 1 % penicillin–streptomycin solution. A passage eight THP-1 monocyte suspension was seeded in a 24-well plate (Corning) at 2 × 10<sup>6</sup> cells/well and differentiated into M0 macrophages. This differentiation was achieved by stimulation with 300 nM phorbol myristate acetate (Sigma-Aldrich), 4 mM L-glutamine (Wako Pure Chemical Corporation), and 500 µM monothioglycerol (Wako Pure Chemical Corporation) for 48 h, and then the cells were incubated in fresh medium for 16 h. M1 macrophages were prepared using the following methods. A passage eight THP-1 monocyte suspension was seeded in a 24-well plate (Corning) at 2 × 10<sup>6</sup> cells/well. This suspension was stimulated with 100 nM phorbol myristate acetate, 4 mM L-glutamine, and 500 nM monothioglycerol for 72 h for differentiation into macrophages, and then the cells were incubated in fresh medium for 24 h. The cells were then further stimulated with 20 ng/mL interferon-gamma (Wako Pure Chemical Corporation) and 10 pg/mL lipopolysaccharide ([LPS] Wako Pure Chemical Corporation) for 24 h and then incubated in fresh medium for 16 h. M0 and M1 macrophages were maintained in Advanced RPMI 1640 containing 1 % fetal bovine serum and a 1 % penicillin–streptomycin solution. The macrophages were exposed to 500 µL of TPM or ACM samples or MV2 medium with 1 % DMSO for 1 h. After the exposure, the medium was replaced with 1800 µL of MV2 medium. After 3 h of incubation, the medium was collected and centrifuged at 1000 × g for 5 min, and the supernatant was collected as conditioned medium for each sample and stored at – 80 °C until testing (see also an overview of the procedure in our previous study) (Ohashi, 2023).

#### RNA preparation

Endothelial tubules were exposed directly/indirectly to tobacco samples or positive (100 pg/mL tumor necrosis factor [TNF]-α and 100 pg/mL interleukin [IL]-1β)/negative control (MV2 medium with 1 % DMSO) samples (Table 1) and incubated on a rocker for 24 h. After the exposure, the tubules were washed with MV2 medium, and an RNeasy Plus Mini Kit (Qiagen, Hilden, Germany) and QIAshredder (Qiagen) were used to isolate RNA in accordance with the manufacturer's instructions as follows. A total of 100 µL of Buffer RLT Plus with 40 mM dithiothreitol (Wako Pure Chemical Corporation) was applied to each chip. After a few pipetting to disrupt the endothelial cells, the lysate was collected from four chips of the same exposure condition to a microcentrifuge tube. The lysate was vortexed for 10 s to ensure that no cell clumps were visible. The lysate was then placed in a QIAshredder spin

**Table 2**

Differentially expressed genes identified in each exposure sample. Differentially expressed genes were detected using an absolute log<sub>2</sub> fold change > 1 and an FDR < 0.1 as analysis-ready molecules in IPA software.

	1R6F			DT3.0a		
	100 µg/ mL	200 µg/ mL	400 µg/ mL	200 µg/ mL	1000 µg/ mL	3000 µg/ mL
Direct	693	3026	2785	67	393	2272
Indirect M0	252	270	306	58	62	93
Indirect M1	47	74	29	7	8	10

column and centrifuged at  $10,000 \times g$  for 2 min to homogenize. The homogenized lysate was transferred to a 2-mL collection tube and placed in a gDNA Eliminator spin column and centrifuged at  $10,000 \times g$  for 30 s. A total of 350 µL of 70 % ethanol (Wako Pure Chemical Corporation) was added to the saved flow-through and mixed well by pipetting. This flow-through including any precipitate was transferred to a 2-mL collection tube, placed in an RNeasy spin column, and centrifuged at  $10,000 \times g$  for 15 s, and the flow-through was discarded. A volume of 700 µL of Buffer RW1 was added to the RNeasy spin column and centrifuged at  $10,000 \times g$  for 15 s. After this centrifugation, 500 µL of Buffer RPE, which was diluted by a four times volume of 99.5 % ethanol (Wako Pure Chemical Corporation), was added to the RNeasy spin column and centrifuged at  $10,000 \times g$  for 15 s. Another 500 µL of Buffer RPE was added and centrifuged at  $10,000 \times g$  for 2 min. A new 1.5-mL collection tube was placed in the RNeasy spin column, and 40 µL RNase-free water was directly added to the spin column membrane and centrifuged at  $10,000 \times g$  for 1 min to elute the RNA. The purified RNA was stored at  $-80 \text{ }^\circ\text{C}$  until RNA-seq analysis.

#### Rna-seq and data analysis

Purified RNA was resuspended in Clontech buffers for mRNA amplification (TaKaRa Bio, Kyoto, Japan) by 5' template-switching

polymerase chain reaction with a Clontech SMART-Seq v4 Ultra Low Input RNA Kit (TaKaRa Bio) according to the manufacturer's instructions. The amplified cDNA was fragmented and linked with dual-indexed barcodes using Illumina Nextera XT DNA Library Prep Kits (Illumina Inc., San Diego, CA, USA). The libraries were validated using an Agilent 4200 TapeStation (Agilent Technologies Inc., Santa Clara, CA, USA), and sequenced on the Illumina NovaSeq 6000 platform (Illumina Inc.). RNA-seq was performed by TaKaRa. Genes less than 30 counts were eliminated. The count data were then subjected to the Tag-Count Comparison Graphical User Interface for differential expression analysis. Data normalization and identification of DEGs were performed using the trimmed mean of M values and Deseq2 methods, respectively. DEGs were identified with a corrected p value (False discovery ratio, FDR) < 0.1, and absolute log<sub>2</sub> fold change to the control of each group > 1.0.

#### Pathway-based analysis of altered genes

Pathway analysis with the identified DEGs was performed with Ingenuity pathway analysis (IPA) software (Qiagen). Canonical pathway and "Diseases and Bio functions" analyses were performed using IPA software. The threshold used was an absolute z-score > 2.0 and a corrected Benjamini–Hochberg false discovery rate (FDR) < 0.05 in the canonical pathway analysis with IPA software. When we focused on "cardiovascular disease signaling", only an FDR < 0.05 was applied because the z-score calculation was incompatible in IPA software. In "Diseases and Bio functions" analysis, we used whole categories or "cell death and survival"-related categories in the IPA software. The threshold used in the "Diseases and Bio functions" analyses was an absolute z-score > 2.0 and an FDR < 0.05.

The heatmap of the pathway analysis was generated with R software (Team and R. c. r, 2021) version 4.1.3 or the Excel color scale function.

The libraries used in the analysis with R software were "pheatmap" (Kolde, 2019), "ggplot2" (Wickham, 2009), and "gplots" (Warnes, 2022) packages. Hierarchical clustering was performed with the pheatmap package using the complete linkage method.

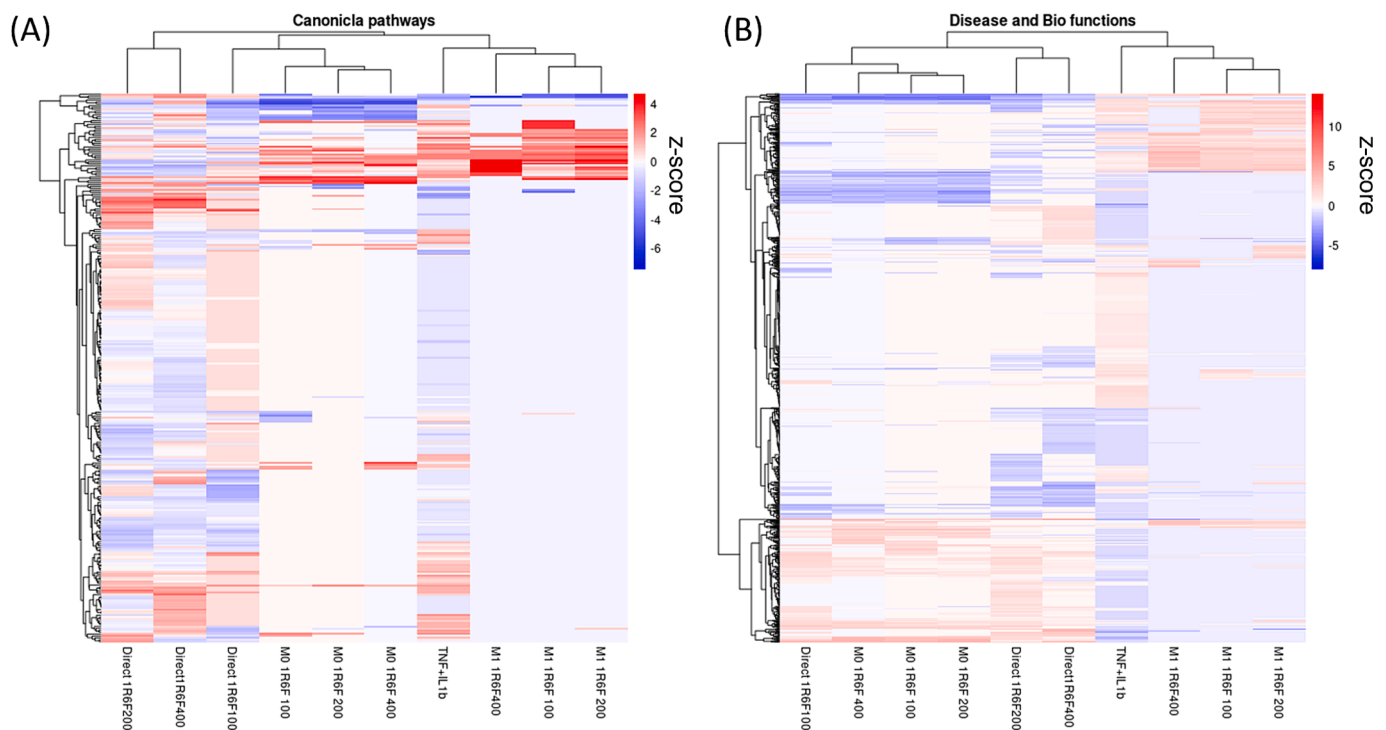


**Fig. 1.** (A) Heatmap of canonical pathway analysis. (B) heatmap of "Diseases and Bio functions" analysis. Hierarchical clustering was performed using R software and the pheatmap library with the complete method.

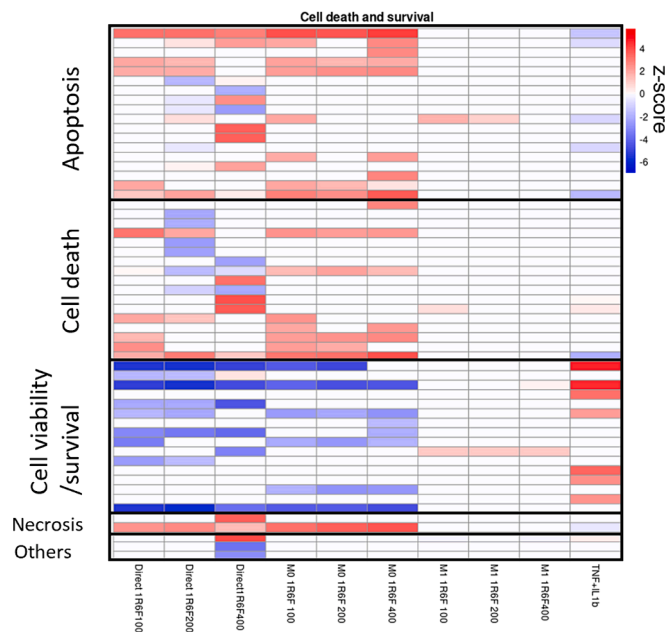


Fig. 2. Heatmap of cell death and survival-related functions in “Diseases and Bio functions.”.

The volcano plot with the DEGs in “Atherosclerosis Signaling” pathway was generated using R software with “ggplot2” package.

### Results and discussion

We first performed a comparative analysis of the transcriptome between direct exposure and indirect exposure of CS-TPM. We found a greater number of DEGs in direct exposure samples than in indirect exposure samples (Table 2), which suggested a greater effect of direct exposure. To further investigate the difference between each exposure condition, we then performed IPA canonical pathway analysis and “Diseases and Bio functions” analysis to identify the relevant pathways and biological functions that were altered by direct or indirect exposure of CS-TPM (Fig. 1). We found that direct exposure and indirect exposure affected canonical pathways differently. In the canonical pathway analysis, direct exposure of CS-TPM, except for the lowest dose, tended to affect various biological pathways differently with typical inflammatory positive control of TNF- $\alpha$  and IL-1 $\beta$ , while indirect exposure caused upregulation of several biological pathways that overlapped with the positive control (Fig. 1A). When we focused on the difference between M0 and M1 indirect exposure, they also showed a different trend (Fig. 1B). Hierarchical clustering showed a consistent result in that indirect exposure via M1 macrophages was closer to the perturbation trend found in the positive control in alteration of the canonical pathways and “Diseases and Bio functions. Indirect exposure via M0 macrophages also showed similar changes to M1 macrophages in canonical

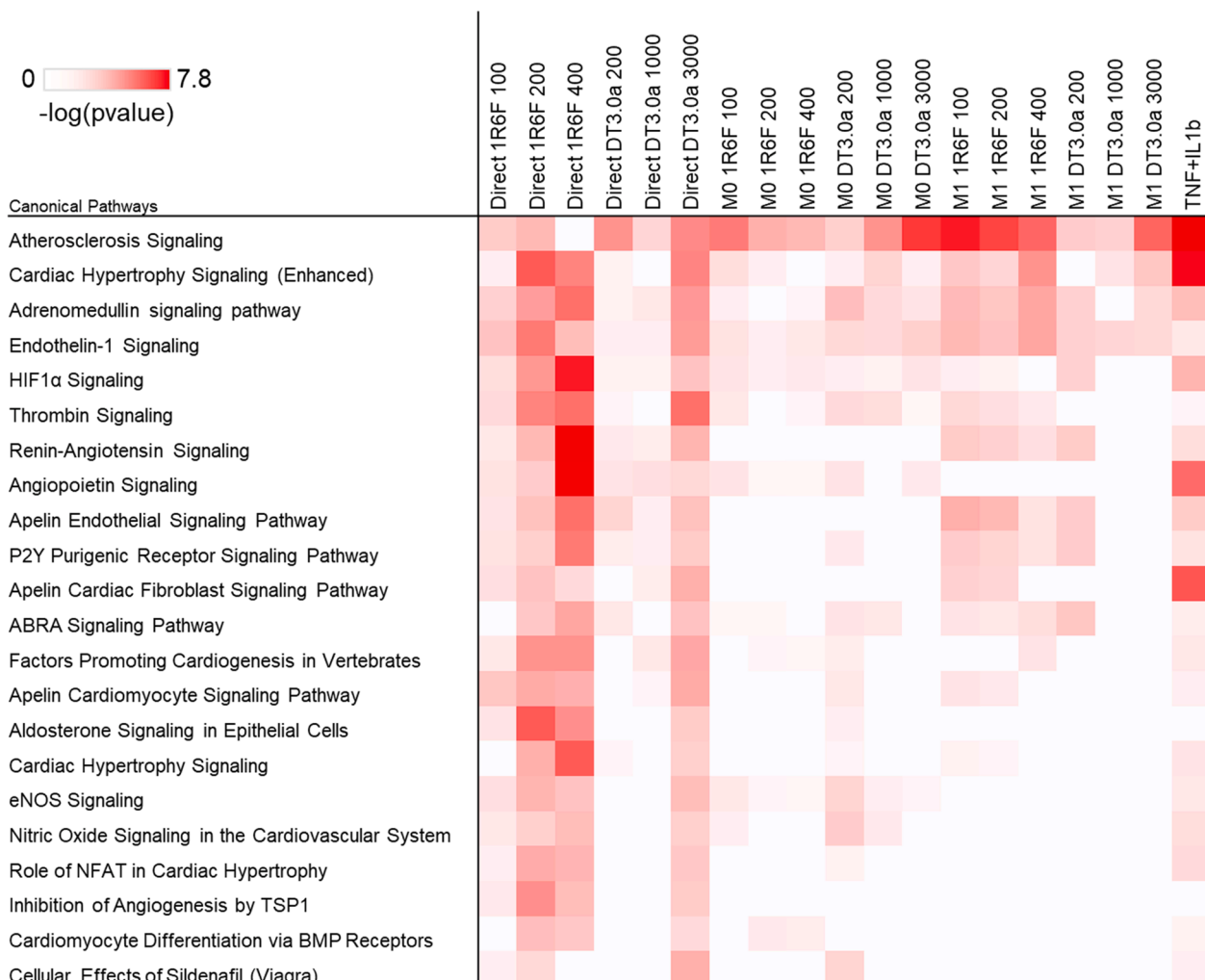
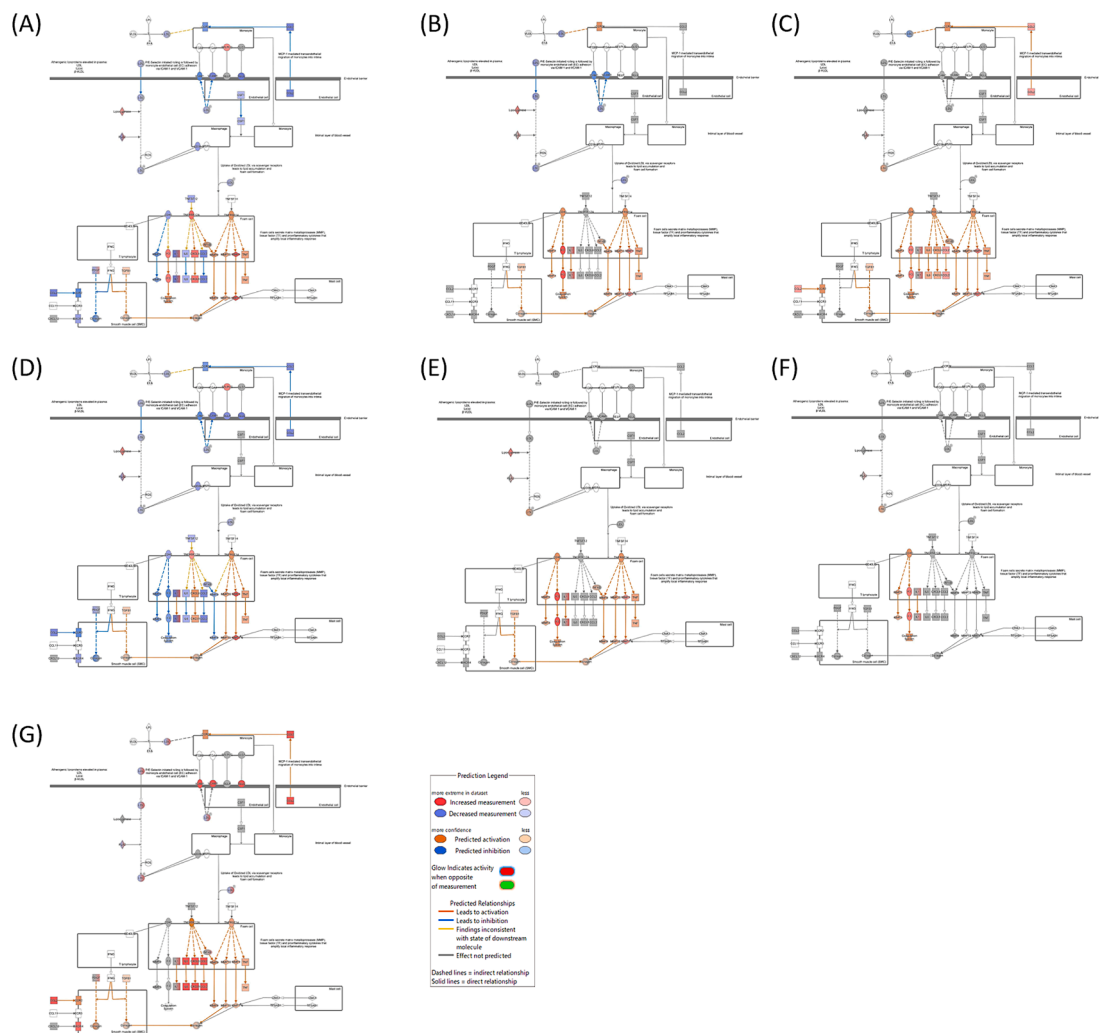


Fig. 3. Heatmap of cardiovascular signaling pathways in IPA software. Canonical pathways are sorted in order of  $-\log(p\text{ value})$ . IPA; Ingenuity Pathway Analysis.



**Fig. 4.** Molecular activity predictor analysis of the “Atherosclerosis signaling” pathway. (A) Direct exposure of 200 µg/mL CS-TPM. (B) Indirect exposure of 100 µg/mL CS-TPM via M0 macrophages. (C) Indirect exposure of 100 µg/mL CS-TPM via M1 macrophages. (D) Direct exposure of 3000 µg/mL DT3.0a-ACM. (E) Indirect exposure of 3000 µg/mL DT3.0a via M0 macrophages. (F) Indirect exposure of 3000 µg/mL DT3.0a-ACM via M1 macrophages. (G) Direct exposure of TNF-α and IL-1β. Samples that showed the lowest p value in each group were selected. A large-scale version of each figure and samples at the other doses is shown in the Supplementary figures. CS; cigarette smoke, TPM; total particulate matter, DT3.0a; Direct Heating Tobacco System Platform 3 Generation 3 version a, ACM; aerosol collected mass, TNF; tumor necrosis factor, IL; interleukin.

pathways, but it was similar to the direct exposure method when “Diseases and Bio functions” was focused on. TNF-α and IL-1β are inflammatory mediators. Therefore, an alteration of biological pathways in TNF-α and IL-1β exposure represents inflammatory responses in endothelial cells. M1 macrophages also play a crucial role in atherogenesis as pro-inflammatory mediators (Moore et al., 2013; Wu, 2023). Therefore, indirect exposure of CS-TPM via M1 macrophages could successfully represent inflammatory conditions via endothelial-immune cell communication under CS exposure. In contrast, the analysis on “cell death and survival”-related biological functions in IPA software showed that direct exposure samples showed positive and negative changes in cell death-related gene categories and survival-related gene categories, respectively (Fig. 2). This finding suggests cell damage is a dominant effect in direct exposure. Indirect exposure via M0 macrophages showed similar patterns of changes in cell death-related pathways, while indirect exposure via M1 macrophages did not show noticeable changes in this category.

To perform more in-depth investigation, canonical pathway analysis with “cardiovascular disease signaling” in IPA software was performed. We found that direct exposure and indirect exposure appeared to significantly affect the “Atherosclerosis Signaling” pathway (Fig. 3). We

further investigated changes in this pathway with the Molecular Activity Predictor function of IPA. The Molecular Activity Predictor function is able to predict up- or downregulation of unobserved genes in the pathways of interest on the basis of the observed DEGs. Therefore, this function provides insight into the active state of the pathway. We found that most of the genes annotated in the “Atherosclerosis Signaling” pathway were observed or predicted downregulated genes in the direct exposure samples (Fig. 4A and Supplementary figures). In contrast, various genes in the “Atherosclerosis Signaling” pathway were upregulated or predicted upregulated in the indirect exposure samples (Fig. 4B and C), especially via the M1 subtype. While various factors contribute to the pathogenesis of CVD, our result suggests that the indirect exposure method is suitable for reproducing inflammatory inter-cellular communication between tissue-resident macrophages and VECs which is involved in CVD development (Laratta and van Eeden, 2014). Pseudo-culture with M0 and M1 macrophages represented atherogenic alterations in VECs, but to a different extent. This finding could reflect the difference between healthy individuals with steady-state macrophage dominance and individuals with hyperlipidemia or any other inflammatory condition who could have pro-inflammatory M1 subtype dominance in lung tissue (Aegerter et al., 2022).

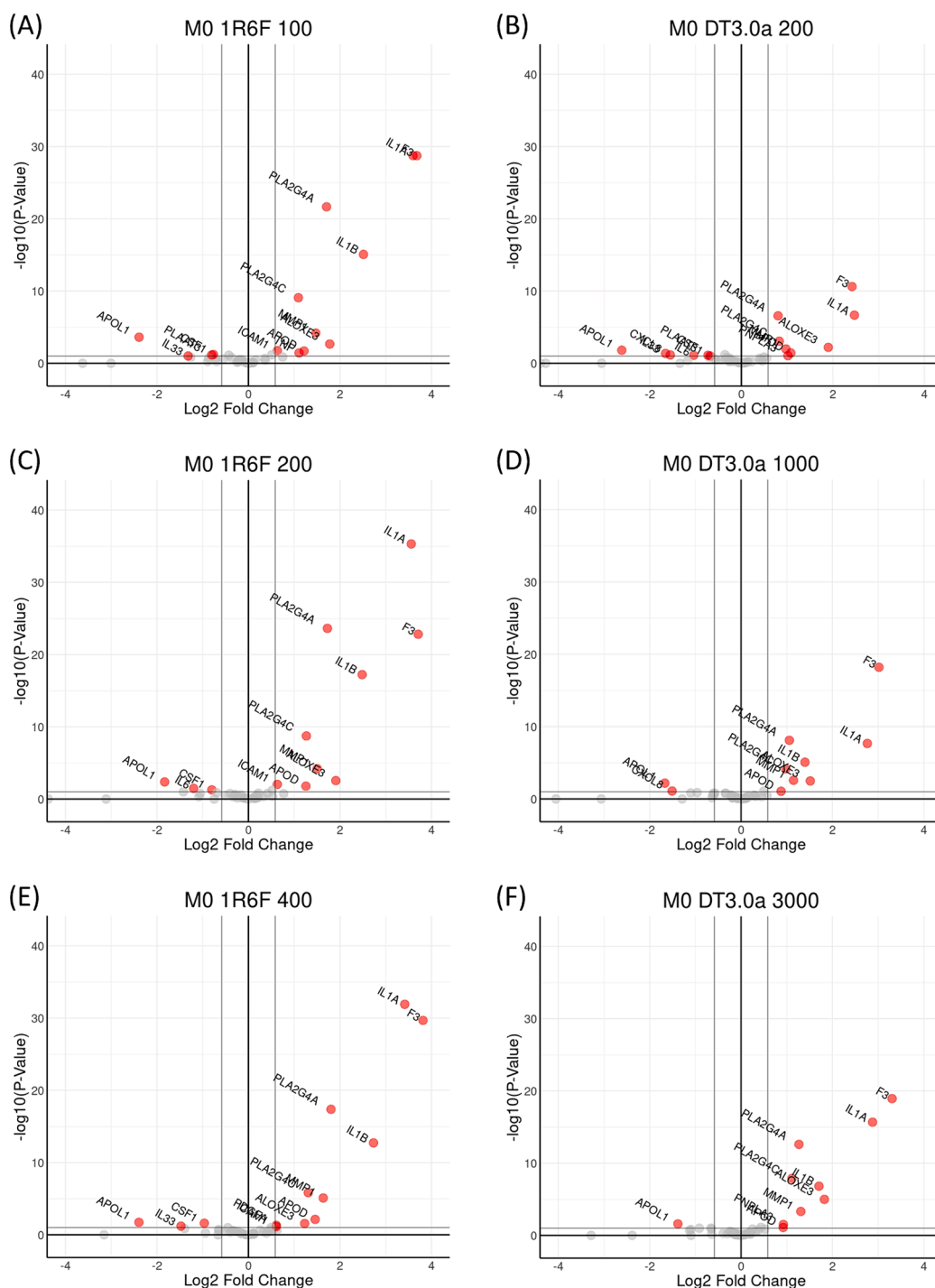


**Fig. 5.** Volcano plot of DEGs in the “Atherosclerosis signaling” pathway from pseudo-co-culture of vascular-on-a-chip and M0 macrophages. (A), (C), and (E) Indirect exposure of 100, 200, and 400  $\mu\text{g/mL}$  CS-TPM. (B), (D), and (F) Indirect exposure of 200, 1000, and 3000  $\mu\text{g/mL}$  DT3.0a-ACM. The threshold was a  $-\log_{10}$  p value  $> 1$  and  $|\log_2$  fold change  $> 0.58$ . DEGs; differentially expressed genes, CS; cigarette smoke, TPM; total particulate matter, DT3.0a; Direct Heating Tobacco System Platform 3 Generation 3 version a, ACM; aerosol collected mass.

We also performed a comparative analysis of the transcriptome between vascular-on-a-chip exposed to CS-TPM and vascular-on-a-chip exposed to DT3.0a-ACM indirectly via M0 or M1 macrophages. Aerosol generated from HTPs generally contain less and fewer HPHCs than CS (Hashizume, 2023). Therefore, we expected that DT3.0a-ACM would show less pronounced effects than CS-TPM. As expected, indirect exposure of DT3.0a-ACM to vascular-on-a-chip showed a smaller number of DEGs than that of CS-TPM to this chip when compared at comparable concentrations (Table 2). This finding was observed even with

the presence of a preexisting inflammatory condition by pseudo-co-culture with M1 macrophages. Similar to CS-TPM, the pathways affected by DT3.0a-ACM, in canonical pathway analysis with “cardiovascular disease signaling” in IPA software, was the “Atherosclerosis Signaling” pathway (Fig. 3) with the lowest or very low p value. However, the number of upregulated and predicted upregulated genes with DT3.0a-ACM was less than that with CS-TPM (Fig. 4E and F). When we focused on the DEGs in the “Atherosclerosis Signaling” pathway, DT3.0a-ACM had less effect than CS-TPM with indirect exposure via M0

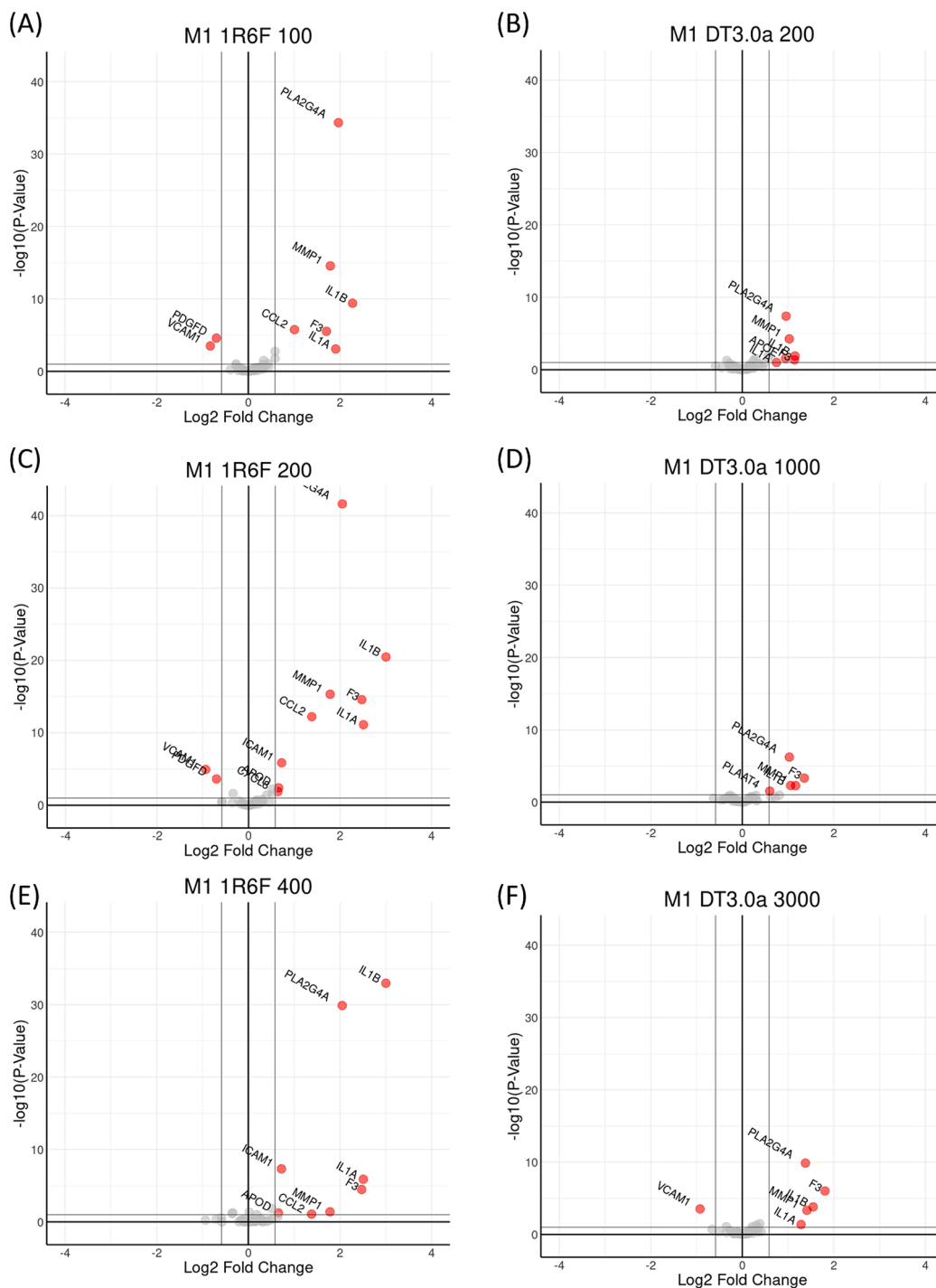


**Fig. 6.** Volcano plot of DEGs in the “Atherosclerosis signaling” pathway from pseudo-co-culture of vascular-on-a-chip and M1 macrophages. (A), (C), and (E) Indirect exposure of 100, 200, and 400  $\mu\text{g}/\text{mL}$  CS-TPM. (B), (D), and (F) Indirect exposure of 200, 1000, and 3000  $\mu\text{g}/\text{mL}$  DT3.0a-ACM. The threshold was a  $-\log_{10}$  p value  $> 1$  and  $|\log_2$  fold change  $> 0.58$ . DEGs; differentially expressed genes, CS; cigarette smoke, TPM; total particulate matter, DT3.0a; Direct Heating Tobacco System Platform 3 Generation 3 version a, ACM; aerosol collected mass.

and M1 macrophages (Figs. 5 and 6). Particularly, even at the highest dose of DT3.0a-ACM, which was a 7.5–30-fold higher concentration than CS-TPM, indirect exposure via M1 macrophages showed less pronounced effects on this pathway than CS-TPM. These results suggest that, even if there is already an inflammatory condition, DT3.0a-ACM does not exacerbate atherosclerotic conditions further. Overall, there appears to be weaker biological activity of DT3.0a-ACM than CS-TPM, and this could explain the reduced-risk potential of DT3.0a.

Based on our previous report, we found that our vascular-on-a-chip

system was able to detect increased expression of an adhesion molecule and monocyte-endothelial adhesion, which are known important biological events in the early stage of atherosclerosis, by TNF- $\alpha$  and IL-1 $\beta$  at concentrations ranging from 25 to 400  $\text{pg}/\text{mL}$  (Ohashi, 2023). This concentration range is lower than the typical range of these cytokines (i. e., 1–10  $\text{ng}/\text{mL}$ ) in the other *in vitro* test systems (Diaz, 2023; Chen, 2023; Wang, 2020). In addition, the blood concentration of these cytokines in CVD patients is known to be less than 100  $\text{pg}/\text{mL}$  (25  $\text{pg}/\text{mL}$  or less in typical) (Almassabi, 2023; Shademan, 2021; Ridker, 2000).



Therefore, our vascular-on-a-chip system could have clinically relevant sensitivity to observe CVD-related endpoints. Result of the current study supports this hypothesis that indirect exposure of vascular-on-a-chip to CS-TPM, which induces those proinflammatory cytokines secretion in the range of 20–100 pg/mL (Ohashi, 2023), showed transcriptomic perturbation related to atherosclerosis signaling pathway.

## Limitations

While we successfully demonstrated the importance of macrophages in the pathogenesis of CVD *in vitro*, there are several limitations to this study. First, because our *in vitro* test system aimed to explore the potential effects of tobacco product emissions on atherogenesis as a form of acceleration study, the exposure concentrations could not be aligned with the actual exposure concentration in human use scenarios. Esther Jr et al. estimated airway nicotine concentration in the airway is 70–850 ng/mL, and Benowitz et al. summarized that nicotine concentration of arterial blood in current smokers is 20–60 ng/mL (Esther, 2023; Benowitz et al., 2009). Meanwhile, the calculated nicotine concentration used in the current study was ranging from 4.2 to 17.2 µg/mL for CS-TPM and 6.3–94 µg/mL for DT3.0a-ACM, respectively, based on our previous study (Hashizume, 2023). Therefore, applying weaker but longitudinal exposure could be a next step for reproducing more human relevant situations. Second, we indirectly exposed CS-TPM or DT3.0a-ACM via macrophages. However, when considering the real-world exposure scenario, inhaled substances should be exposed to and metabolized in lung epithelial cells first. In addition, there are various subtypes of macrophages and other types of immune cells in lung tissue. Cell-cell communication among those tissue-resident cells contributes to maintaining homeostasis and to the pathogenesis of atherosclerosis. Incorporation of these processes in our model system would improve its relevance to the human situation. Furthermore, disease modeling with experimental animals typically uses a high-fat diet to induce atherosclerosis, but such a condition has not yet been reproduced in our *in vitro* test system. Direct representation of the blood conditions (i.e., hyperlipidemia) in an *in vitro* test system could further improve its relevance to the human body.

## Conclusions

In this study we demonstrated the suitability of our *in vitro* vascular-on-a-chip system for mimicking early-stage atherosclerosis by transcriptomic analyses. To the best of our knowledge, we believe that our test system is the first *in vitro* model intended to recapitulate the cell–cell communication between immune cells in the lung space and vascular endothelial cells. Incorporating M1 macrophages into the vascular-on-a-chip system represented the inflammatory condition and could enhance the *in vitro* recapitulation of atherogenesis related to inhalable substances. Under both the steady-state (i.e., pseudo-co-culture with M0 macrophages) and inflammatory conditions (i.e., pseudo-co-culture with M1 macrophages), there appears to be weaker biological activity of DT3.0a-ACM than CS-TPM in atherosclerosis, suggesting reduced risk potential of DT3.0a. Whilst the reduced risk potential of HTPs in the context of atherosclerosis is still not fully understood, thus further developments of risk assessment methods for late-stage atherosclerosis are desirable.

## Funding

Japan Tobacco Inc. was the sole source of funding for this project. No external sources of funding were used for this project.

## Declaration of competing interest

The authors declare the following financial interests/personal relationships which may be considered as potential competing interests:

Shigeaki Ito reports a relationship with Japan Tobacco Inc that includes: employment. Kazuhiro Ohashi reports a relationship with Japan Tobacco Inc that includes: employment. Ayaka Hayashida reports a relationship with Japan Tobacco Inc that includes: employment. Atsuko Nozawa reports a relationship with Japan Tobacco Inc that includes: employment. The work involved a DT3.0a (Ploom X, manufactured by Japan Tobacco Inc.) If there are other authors, they declare that they have no known competing financial interests or personal relationships that could have appeared to influence the work reported in this paper.

## Data availability

Data will be made available on request.

## Acknowledgments

The authors are grateful to Dr. Takashi Sekine, Dr. Yuichi Furudono and Dr. Hitoshi Fujimoto for their supports in conducting this study. We thank Ellen Knapp, PhD, from Edanz (<https://jp.edanz.com/ac>) for editing a draft of this manuscript.

## References

- Aegerter, H., Lambrecht, B.N., Jakubzick, C.V., 2022. Biology of lung macrophages in health and disease. *Immunity* 55 (9), 1564–1580.
- Almassabi, R.F., et al., 2023. Differential expression of serum proinflammatory cytokine TNF-α and genetic determinants of TNF-α, CYP2C19\*17, miR-423 genes and their effect on Coronary artery disease predisposition and progression. *Life (basel)* 13 (11), p2142.
- Benowitz, N.L., Hukkanen, J., Jacob 3rd., P., 2009. Nicotine chemistry, metabolism, kinetics and biomarkers. *Handb Exp Pharmacol.* 192, 29–60.
- Borger, J.G., 2020. Spatiotemporal Cellular networks maintain immune homeostasis in the lung. *EMJ Respir* 8 (1).
- Chen, L., et al., 2023. Inducible nitric oxide synthase activity mediates TNF-α-induced endothelial cell dysfunction. *Am J Physiol Cell Physiol* 325 (3), C780–C795.
- Dempsey, R., et al., 2023. Preliminary toxicological assessment of heated tobacco products: a review of the literature and proposed strategy. *Toxicol Rep* 10, 195–205.
- Diaz, S.L., et al., 2023. TNF-α-mediated endothelial cell apoptosis is rescued by hydrogen sulfide. *Antioxidants (basel)*. 12 (3), 734.
- Esther Jr, C.R., et al., 2023. Prolonged, physiologically relevant nicotine concentrations in the airways of smokers. *Am J Physiol Lung Cell Mol Physiol* 324 (1), L32–L37.
- Food and Drug Administration, *Modified Risk Tobacco Product Applications DRAFT GUIDANCE*. 2012.
- Food and Drug Administration. *Modified Risk Granted Orders*. 2023; Available from: <https://www.fda.gov/tobacco-products/advertising-and-promotion/modified-risk-granted-orders>.
- Food and Drug Administration, *Harmful and Potentially Harmful Constituents in Tobacco Products and Tobacco Smoke; Established List*. 2012.
- Forster, M., et al., 2018. Assessment of novel tobacco heating product THP1.0. Part 3: comprehensive chemical characterisation of harmful and potentially harmful aerosol emissions. *Regul Toxicol Pharmacol* 93, 14–33.
- Gimbrone Jr., M.A., Garcia-Cardena, G., 2016. Endothelial cell dysfunction and the pathobiology of atherosclerosis. *Circ Res* 118 (4), 620–636.
- Gould, N.S., et al., 2011. Lung glutathione adaptive responses to cigarette smoke exposure. *Respir Res* 12 (1), 133.
- Hashizume, T., et al., 2023. Chemical and *in vitro* toxicological comparison of emissions from a heated tobacco product and the 1R6F reference cigarette. *Toxicol Rep* 10, 281–292.
- Horinouchi, T., et al., 2020. Cigarette smoke Extract and its cytotoxic factor acrolein inhibit nitric oxide production in human Vascular endothelial cells. *Biol Pharm Bull* 43 (11), 1804–1809.
- Hou, F., et al., 2021. Diversity of macrophages in lung homeostasis and diseases. *Front Immunol* 12, 753940.
- Kolde, R. *pheatmap: Pretty Heatmaps. R package version 1.0.12*. 2019; Available from: <https://CRAN.R-project.org/package=pheatmap>.
- Kotlyarov, S., 2023. The role of smoking in the mechanisms of development of chronic obstructive Pulmonary disease and atherosclerosis. *Int J Mol Sci* 24 (10).
- Laratta, C.R., van Eeden, S., 2014. Acute exacerbation of chronic obstructive pulmonary disease: cardiovascular links. *Biomed Res Int* 2014, 528789.
- Lesgards, J.F., et al., 2002. Assessment of lifestyle effects on the overall antioxidant capacity of healthy subjects. *Environ Health Perspect* 110 (5), 479–486.
- Libby, P., et al., 2019. *Atherosclerosis Nature Reviews Disease Primers* 5, 1.
- Lugg, S.T., et al., 2022. Cigarette smoke exposure and alveolar macrophages: mechanisms for lung disease. *Thorax* 77 (1), 94–101.
- Mishra, M., Prasad, K., 2022. Mechanism of hypercholesterolemia-induced atherosclerosis. *Rev. Cardiovasc. Med.* 23 (6).
- Moore, K.J., Sheedy, F.J., Fisher, E.A., 2013. Macrophages in atherosclerosis: a dynamic balance. *Nat Rev Immunol* 13 (10), 709–721.

- Muratani, S., et al., 2023. Oxidative stress-mediated epidermal growth factor receptor activation by cigarette smoke or heated tobacco aerosol in human primary bronchial epithelial cells from multiple donors. *J Appl Toxicol* 43 (9), 1347–1357.
- Obad, A., et al., 2018. Alcohol-mediated organ damages: Heart and brain. *Front Pharmacol* 9, 81.
- Ohashi, K., et al., 2023. Human vasculature-on-a-chip with macrophage-mediated endothelial activation: the biological effect of aerosol from heated tobacco products on monocyte adhesion. *Toxicol in Vitro* 89, 105582.
- Ou, H., et al., 2017. The Characteristics and roles of advanced oxidation protein products in atherosclerosis. *Cardiovasc Toxicol* 17 (1), 1–12.
- Phillips, B., et al., 2019. A six-month systems toxicology inhalation/cessation study in ApoE(-/-) mice to investigate cardiovascular and respiratory exposure effects of modified risk tobacco products, CHTP 1.2 and THS 2.2, compared with conventional cigarettes. *Food Chem Toxicol* 126, 113–141.
- Poussin, C., et al., 2016. Systems toxicology-based assessment of the candidate modified risk tobacco product THS2.2 for the adhesion of monocytic cells to human coronary arterial endothelial cells. *Toxicology* 339, 73–86.
- Rafeian-Kopaei, M., et al., 2014. Atherosclerosis: process, indicators, risk factors and new hopes. *Int J Prev Med* 5 (8), 927–946.
- Ridker, P.M., et al., 2000. Elevation of Tumor Necrosis Factor- $\alpha$  and Increased Risk of Recurrent Coronary Events after Myocardial Infarction. 101, 2149–2153.
- Saha, P., et al., 2023. The effects of dual IQOS and cigarette smoke exposure on airway epithelial cells: implications for lung health and respiratory disease pathogenesis. *ERJ Open Res* 9 (3).
- Salekeen, R., et al., 2022. Lipid oxidation in pathophysiology of atherosclerosis: current understanding and therapeutic strategies. *Int J Cardiol Cardiovasc Risk Prev* 14, 200143.
- Sekine, T., et al., 2019. Regulation of NRF2, AP-1 and NF- $\kappa$ B by cigarette smoke exposure in three-dimensional human bronchial epithelial cells. *J Appl Toxicol* 39 (5), 717–725.
- Shademan, B., et al., 2021. Exploring potential serum levels of homocysteine, interleukin-1 beta, and apolipoprotein B 48 as new biomarkers for patients with ischemic stroke. *J Clin Lab Anal* 35, e23996.
- Shi, H., Liu, J., Gao, H., 2021. Benzo(a)pyrene induces oxidative stress and inflammation in human vascular endothelial cells through AhR and NF- $\kappa$ B pathways. *Microvasc Res* 137, 104179.
- Team, R.C. R: A language and environment for statistical computing. R Foundation for Statistical Computing, Vienna, Austria. 2021; Available from: <https://www.r-project.org/>.
- Wang, B., et al., 2020. A comparative study unraveling the effects of TNF- $\alpha$  stimulation on endothelial cells between 2D and 3D culture. *Biomed Mater* 15, 065018.
- Gregory R. Warnes, B.B., Lodewijk Bonebakker, Robert Gentleman, Wolfgang Huber, Andy Liaw, Thomas Lumley, Martin Maechler, Arni Magnusson, Steffen Moeller, Marc Schwartz and Bill Venables, *gplots: Various R Programming Tools for Plotting Data. R package version 3.1.3.* 2022.
- Wickham, H. *ggplot2: Elegant Graphics for Data Analysis.* . 2009 [cited 2016].
- World Health Organization. *Global health estimates: Leading causes of death.* 2020; Available from: <https://www.who.int/data/gho/data/themes/mortality-and-global-health-estimates/gho-leading-causes-of-death>.
- Wu, J., et al., 2023. Macrophage polarization states in atherosclerosis. *Front Immunol* 14, 1185587.
- Yang, D.C., Chen, C.H., 2018. Cigarette smoking-mediated macrophage reprogramming: mechanistic insights and therapeutic implications. *J Nat Sci* 4 (11).
- Zhou, Y., et al., 2022. Acrolein evokes inflammation and autophagy-dependent apoptosis through oxidative stress in vascular endothelial cells and its protection by 6-C-(E-2-fluorostyryl)naringenin. *J. Funct. Foods* 98.